Theoretical investigation of the excitation of leaky modes for multi-layered models

Bo Wu[1, 2, 3], Caiwang Shi[2], Xiaofei Chen[2], and Qi Zhang[1]

[1]Peng Cheng Laboratory, Shenzhen, China, [2]Department of Earth and Space Sciences, Southern University of Science and Technology, Shenzhen, China, [3]College of Civil Engineering & Architecture, China Three Gorges University, Yichang, China

*Corresponding author：Bo Wu (wubolion@mail.ustc.edu.cn)

Key Points:

- The excitation of leaky modes is thoroughly investigated.
- Accurate computation of leaky modes gives us a clear physical picture of the two types of leaky modes.
- The attenuation diagram and the eigen-displacements of leaky modes serve as the basis to invert the P-wave velocity structure.

Abstract

With the advent of the array-based methods, the observations of leaky modes from earthquake records and ambient noise are frequently reported. It is urgently needed to have an effective guide to the selection of certain leaky modes to put into practical inversion combined with other imaging methods. To this end the excitation of leaky modes for multi-layered models is theoretically investigated. By computing theoretical seismograms for different source mechanisms and different source depths with the discrete wavenumber method and the normal-mode summation method separately, the contribution of leaky modes to the resultant seismograms is qualitatively evaluated and the effect of the source depth for the same source mechanism is in detail examined. Further, we perform accurate computation of leaky modes for two models and categorize the leaky modes into PL and OP (organ-pipe) modes, whose distinctive properties are characterized both from the attenuation and from the eigen-displacements of these two types of modes. Also, these results could help explain very well the occurrence of certain leaky modes on the dispersion spectrum and be indicative of the reasonable choice of certain leaky modes to put them into practical inversion for P-velocity structures.

Plain Language Summary:

The leaky modes, unlike the normal modes, attenuate exponentially with time because of leakage to the underlying substratum, and are frequently observed from earthquake records and ambient noise with the advent of the array-based methods. Since the leaky modes have long been felt to be able to provide complementary information to constrain compressional-wave velocity just as the normal modes are used to invert only the shear-wave velocity, an effective guide is thus urgently needed to help select certain portion of leaky modes to put into practical inversion together with other imaging methods. To this end, the excitation of leaky modes for stratified

models is theoretically investigated. Our results could help explain very well the occurrence of certain portion of leaky modes on the dispersion diagram and why massive theoretically computed leaky modes do not appear at the same time. With the aid of the results of the attenuation and the eigen-displacements of leaky modes, the leaky modes can be reasonably selected to perform joint inversion to obtain compressional-wave velocity structure.

1. Introduction

Recently, a great interest in leaky modes arises and consequent studies have been undertaken both from theoretical and observational or application perspectives (Furumura and Kennett, 2018; Znak et al., 2015; Gao et al., 2014; Wu and Chen, 2017; Ma et al., 2019; García-Jerez and Sánchez-Sesma, 2015; Li et al., 2021; Li et al., 2022). Leaky modes physically describe travelling disturbances that leak at least S waves into the substratum. Since the PL wave (Sommville, 1930), a long period (> 10 s) wave train beginning shortly after the initial P wave, was first identified with the fundamental leaky mode (Oliver and Major, 1960), subsequent observations of wave trains which can be interpreted in terms of leaky modes had been reported (Oliver, 1961, 1964; Gilbert and Laster, 1962; Su and Dorman, 1965). During the same stage, the theory of leaky modes had also experienced a series of developments (Rosenbaum, 1960; Phinney, 1961; Gilbert, 1964; Watson, 1972), and later the computation of complete synthetic seismograms by mode summation was also completed (Haddon, 1984, 1986, 1987).

Leaky modes have long been suggested be used to constrain P-wave velocity structure and been thought to have unique advantages where traditional surface waves and classic seismic reflection and refraction methods may fall short (Oliver and Major, 1960; Su and Dorman, 1965; Roth et al., 1998). On the way to putting leaky modes into practical inversion, earlier studies had been devoted to the effects of the crustal structure and P-wave velocity structure on the leaky modes (Haskell, 1966; De Bremaecker, 1967; Cochran et al., 1970; Stalmach and De Bremaecker, 1973; Su and Dorman, 1965) and to the attenuation and the excitation of the leaky modes (Laster et al., 1965; Haskell, 1966; Dainty, 1971) and found that a deeper event in the crust could more efficiently excite the fundamental leaky mode (the most commonly seen mode) than a near-surface source (Dainty, 1971). Notwithstanding these progresses after 1960, leaky modes have found limited applications in imaging underground structures (Su and Dorman, 1965; Ibrahim, 1969; Fujita and Nishimura, 1991) and have been approximately computed in the case of high Poisson's ratios (Roth et al., 1998; Roth and Holliger, 1999; Boiero et al., 2013; Gao et al., 2014).

Given the above observation of applications of leaky modes, the accurate computation of them may be one limiting factor in incorporating leaky modes into practical inversion. Furthermore, it is found in the published papers that, the computed leaky modes are much more than the actual appearance of them in the dispersion spectrum (Li et al., 2021; Wu and Chen, 2017; Roth et al., 1998). Then two questions need to be answered in this study: a) what kind of conditions may favor the excitation of the leaky modes, which requires considering the effects of the source and the media properties but restricts herein to the study of the former factor only; b) why massive leaky modes are not observed in the dispersion spectrum, which needs to be considered by integrating the attenuation of leaky modes with their eigen-displacements. We wish by answering these two questions the realistic inversion for velocity structures using leaky modes might be laid on a solid theoretical foundation. The outline of this paper is as follows: we first make two inferences on the leaky modes based on the formulae for independently synthesizing seismograms and then introduce the method and the strategy of accurately computing leaky modes in Section Theory and Methods; the contribution of leaky modes to the seismograms and the effects of the source on the excitation of leaky modes are illustrated in Section Results and Analysis, and the dispersive calculations of leaky modes together with the attenuation and the eigen-displacements of leaky modes are also shown for two cases in this Section, with a careful analysis being performed to explain the resultant theoretical dispersion spectrum; lastly, summarizing the main results of our investigation, a detailed conclusion is given in the concluding section.

2. Theory and Methods

2.1 Inferences on the leaky modes

We can evaluate the effect of leaky modes on the seismograms from two different synthetic methods: the discrete wavenumber method (DWM) (Bouchon and Aki, 1977; Chen and Zhang, 2001), by which the seismogram generated is complete, and the normal-mode summation method (NMM) (Aki and Richards, 1980) for synthesizing surface waves only. For the former method, in the cylindrical polar coordinates (r,θ,z), each displacement component of layer j for stratified media consisting of several layers overlying a half space can be expressed in the frequency domain as (Chen, 1999)

$$U^j\left(r,\theta,z;\omega\right) \sim S(\omega)\sum_q R_n(\theta)\int_0^{\infty}\mathrm{K}_q(k,z,\omega;z_s)\cdot J_m(kr)dk\,, \tag{1}$$

where $S(\omega)$ is the source spectra; the summation over q contains q integrals of the multiplication of the Bessel function or its derivative $J_m(kr)(m=0,1,2)$ and the kernel function $\mathrm{K}_q(k,z,\omega;z_s)$ depending on the wavenumber k, the angular frequency ω and the source depth z_s and the receiver depth z; before the integral is the radiation pattern $R_n(\theta)$ with n indicating different radiation types.

For the latter method, taking the Love waves as an example, the displacement excited by the point source $\mathbf{F}\exp(-i\omega t)$ can be expressed as (Aki and Richards, 1980)

$$\begin{aligned}\mathbf{u}^{\mathrm{LOVE}}(r,\theta,z,t) &= \frac{e^{-i\omega t}}{2\pi}\sum_{m=-\infty}^{+\infty}\int_0^{+\infty}(l_1' + l_1''/\Delta(k))\mathbf{T}_k^m(r,\theta)k\,dk \\ &= e^{-i\omega t}\sum_m\sum_n ik_n\frac{l_1''(k_n,m,z,\omega)}{(\partial\Delta/\partial k)_{k=k_n}}\mathbf{T}_{k_n}^{m(1)}(r,\theta)\end{aligned}\,, \tag{2}$$

where $\mathbf{T}_k^m(r,\theta)$ is one of the vector basis functions in the cylindrical system and written as $\mathbf{T}_k^{m(1)}$ with the Bessel function J_m of order m expressed using the Hankel function of the first kind $H_m^{(1)}$, whose explicit expressions and the explanations for the notations l', l'' and the function Δ are referred to Aki and Richards (1980). When k is the eigenvalue k_n, $\Delta(k_n)=0$. $|m| \leq 1$ for the single-force case, and $|m| \leq 2$ for the moment-tensor source.

By scrutinizing Eqs. (1) and (2), we can make two inferences: a) the dispersion spectrum (Wang et al., 2019; Li and Chen, 2020) generated from the kernel function in eq. (1) may correlate with the modal intensity calculated by eq. (2), although the latter relies also on the source mechanism; b) the contribution of leaky modes is just the difference of the seismograms synthesized by the two methods. Experimental evidence will be given in Section III to show the validity of the inferences.

2.2 Computation of leaky modes

The computation of leaky modes for multi-layered models is accomplished in the same manner as that of normal modes of surface waves. The only difference is that, leaky modes are usually complex roots of the dispersion equation while normal modes are real roots, that is, the roots of leaky modes are sought in the complex wavenumber domain for each given frequency, assuming the real ω-complex k approach (Watson, 1972) is adopted. Considering the duality of vertical wavenumber, we may define four Riemann sheets according to the signs of the real parts of the multivalued functions

$$\gamma^{(N+1)} = \sqrt{k^2 - (\omega/\alpha^{(N+1)})^2} \text{ and } \nu^{(N+1)} = \sqrt{k^2 - (\omega/\beta^{(N+1)})^2}, \tag{3}$$

where N is the number of the layers above the half space, whose *P*- and *S*-wave velocities are represented by $\alpha^{(N+1)}$ and $\beta^{(N+1)}$, respectively. The Riemann sheet for which $\mathrm{Re}\{\gamma^{(N+1)}\} > 0$ and $\mathrm{Re}\{\nu^{(N+1)}\} < 0$ is designated as the $(+,-)$ sheet, and similarly the $(-,-)$ sheet means

$\mathrm{Re}\{\gamma^{(N+1)}\} < 0$ and $\mathrm{Re}\{\nu^{(N+1)}\} < 0$. Since the significant contribution to the waveform comes mainly from the $(+,-)$ sheet (Wang and Herrmann, 1980), only the leaky modes in this sheet are computed in our study, which have phase velocities between $\beta^{(N+1)}$ and $\alpha^{(N+1)}$ and describe travelling disturbances leaking only S-wave energy into the substratum.

Built in the framework of the generalized reflection/transmission coefficients method (Chen, 1993; Chen and Chen, 2002; He et al., 2006; Wu and Chen, 2016; Wu and Chen, 2017, 2022), the dispersion equation for solving the leaky modes, identical in form with that for the normal modes, is obtained as

$$\det\{\hat{\mathbf{R}}_{\mathrm{ud}}^{j-1}\hat{\mathbf{R}}_{\mathrm{du}}^{j} - \mathbf{I}\} = 0 \;\; (j = 1, 2, \ldots, N), \tag{4}$$

where $\hat{\mathbf{R}}_{\mathrm{ud}}^{j-1}$ and $\hat{\mathbf{R}}_{\mathrm{du}}^{j}$ are the generalized reflection coefficients associated with the upper and the lower interface in the *j*th layer, and $\mathbf{I}$ is the identity matrix. Note that eq. (4) is a family of secular functions (He et al., 2006; Wu and Chen, 2016), and a thorough search of normal modes for models with fluid layers or abnormal properties may necessarily invoke several secular functions from the family, the left side of eq. (4); however, one suitable dispersion equation may be adequate to find the complex roots of leaky modes (Wu and Chen, 2017).

The direct strategy for searching roots is the grid search in the 2-D complex k-plane, but it turns out time-consuming and yields less accurate results (Roth et al., 1998; Gao et al., 2014). If we resort to some iterative methods such as the Newton-Raphson method, with a series of initial values the roots may be located very efficiently (Gilbert, 1964; Cochran et al., 1970; Watson, 1972; Radovich and De Bremaecker, 1974). Similar to the approach of Watson (1972), we search the roots from high frequency to low frequency, extrapolate the trial value of the root of the same order at the next frequency point, and employ the Newton-Raphson method to achieve the roots to the desired accuracy.

Once all of the leaky roots of the dictated frequency range are found and a check for the mode missing is made, we may then proceed to compute the eigenfunctions of the leaky modes required, in the same manner as that of the normal modes (Wu and Chen, 2016; Wu and Chen, 2022). Numerical examples will be given for two cases in Section III.

3. Results and Analysis

3.1 Contribution of leaky modes to the seismograms

We compute the theoretical seismograms using the DWM and NMM respectively for the crust-upper mantle model (Figure 1) modified from Shen and Ritzwoller (2016). Considering the two source types shown in Table 1, the Green solutions are computed at a distance of 2000 km from the focus of 0.5 km depth and 8 km depth, as shown in Figures 2 and 3, respectively. In both figures, the results for the strike-slip source are labeled as (A) and (B), and those for the dip-slip source are labeled as (C) and (D); the results from the NMM (A, C) are contrasted with that from the DWM (B, D).

We see from Figure 2 that, when the source depth is 0.5 km, the generated synthetic seismograms from the two methods are almost the same, whether for the strike-slip or for the dip-slip source. Figure 3 shows that, however, when the source is 8 km deep, the differences between the seismograms computed from the two methods become very obvious for both of the sources, especially for the strike-slip source. Because the NMM can only synthesize surface waves but the DWM produces complete seismograms including early-arrival body waves, this difference is attributed to the leaky-mode contributions. Therefore, the deeper focus could effectively trigger the *PL* phase on the seismogram, as also observed by Dainty (1971).

3.2 Effects of the source on the excitation of leaky modes

That deep focus could more easily excite leaky modes can also be seen from corresponding dispersion spectra. It can be seen from Figure 4 that, more higher-order leaky modes appear on the dispersion spectrum for the source depth of 8 km than those for the source depth of 0.5 km. Note here that the dispersion spectrum computed from the kernel function depends only on the source depth, the frequency and the wavenumber, with the receiver fixed on the surface, and is blind to different source mechanisms.

We then proceed to study the effects of the source on the excitation of leaky modes in view of the mode intensity. Since the excited strength of normal modes could be easily obtained from eq. (2), the effects of the source on the excitation of normal modes are assumed to have similar effects on the excitation of leaky modes, as will be verified later. Figure 5 gives diagrams of the excited strength of the normal modes for the model shown in Figure 1 for the two types of sources (Table 1) with different source depths. We infer from the results for normal modes that, when the focus depth is shallow (Figures 5A and 5C), the source mechanism has a prominent effect on the excitation of leaky modes, and when the source is deep (Figures 5B and 5D), the effect of the source mechanism seems immaterial. Further, for the same source mechanism, the source depth still has a significant effect on the excitation of leaky modes.

3.3 Case 1: a near-surface model

Using the dispersion equation corresponding to the first layer (cf. eq. (4)), we compute Rayleigh dispersion curves (including normal modes and leaky modes, see Figure 6) for the one-layer half space, a near-surface model (Table 2) proposed by Roth and Holliger (1999). The frequency range is from 10^{-5} to 200 Hz, and the frequency spacing is 1 Hz. Adopting the notation of Watson (1972), the leaky modes computed in the $(+,-)$ Riemann sheet are categorized into two classes: the organ-pipe modes (abbreviated as OP modes) of the relatively steep slope and the PL modes of gentle ramp; the latter could be approximated by acoustic normal modes as shown by blue open circles in Figure 6. It should be pointed out that, due to the essentially different origins of the two types of modes, their phase-velocity curves actually intersect freely one another when the frequency is assumed real, although the modes are connected by lines according to numerical order. Thus this is the distinct pattern of leaky-mode dispersion compared with the well-known avoided-crossing character of normal-mode dispersion curves (Wu and Chen, 2016).

Let us examine then the oscillating character of the two types of modes. We plot the eigen-displacements of PL modes (Figure 7) and OP modes (Figure 8) in the rectangle in Figure 6. Because the eigen-displacements of leaky modes are complex due to their complex horizontal wavenumbers, displayed in Figures 7 and 8 are the real parts of the eigen-displacements, which will not be explicitly stated hereafter. We see from Figure 7 that the energy of the PL modes is mainly concentrated in the region of the 10-m layer thickness and becomes negligibly small as soon as they enter the half space. Therefore, the oscillating character of the PL modes is very similar to that of normal modes. Without taking the attenuation into account, the PL modes contribute significantly to the seismogram when the source is located in layers above the half space. On the contrary, the OP modes have little energy in the first layer but their eigen-displacements grow exponentially in the half space. Consequently, without considering the attenuation, the OP modes are deemed to be difficult to appear on the seismogram when the source is well above the half space. We mention in passing that, although the PL modes in Figure 6 could be approximated by the acoustic normal modes, they have essentially different physical mechanisms, as can be seen by comparing the eigen-displacements of the acoustic modes in Figure 9 with those of the PL modes in Figure 7; obviously, they are dramatically different.

Next, we consider the attenuation of leaky modes. Figure 10 shows that with the increasing frequency the attenuation of each order of leaky mode decreases gradually. Thus, the leaky modes of phase velocities just larger than the maximum shear-wave velocity tend to appear on the dispersion spectrum, as shown in Figure 12. In particular, the three PL modes have extremely small attenuation compared with the rest of the leaky modes, which may account for the more frequent manifestation of the PL modes in near-surface surveys (Roth et al., 1998). The attenuation curves of the three PL modes are specially drawn in Figure 11. It is evident that the three PL modes all display maximas and minimas periodically and that's why the pronounced tuning effect of leaky modes is reported in the literature (Roth et al., 1998; Znak et al., 2015). As a band-pass filter (see Figure 12 for the effect of PL modes), the PL modes may even have wavenumbers with the imaginary parts being almost zero (Figure 11), which, as slowly-attenuating P-SV leaky waves, were extensively studied by García-Jerez and Sánchez-Sesma (2015).

Figure 12 shows the dispersion spectrum for different source depths with the receiver on the free surface. Computed normal modes and leaky modes are in good agreement with the spectrum plotted from the kernel function. Massive OP modes, however, do not appear on the spectrum, partly because their attenuations are relatively larger, and most importantly, they contribute little energy just beneath the surface, as can be seen from the variation of their eigen-displacements with depth (Figure 8). It is clearly revealed from Figure 12 that, with the increasing source depth, the intensity of the excited leaky modes becomes larger, which once again confirms that a deeper seismic event may favor the excitation of leaky modes.

Plotted in Figure 13 are the eigen-displacements of the leaky modes at 180 Hz where there is distinct appearance of leaky modes when the source depth is 15 km. Judging from the oscillating character of leaky modes we have grasped, with the aid of the dispersion diagram (Figure 6), we could more definitely determine which are OP modes and which correspond to PL modes, and explain why some leaky modes are visible on the dispersion spectrum while the others are not.

3.4 Case 2: a shallow-water model

Now let us consider a shallow water model (Table 3), whose maximum *S*-wave velocity is smaller than the *P*-wave velocity in the water. For such a model, due to the observation by Wu et al. (2020) that the dispersion equation is difficult to be used to find any normal modes, the dispersion equation corresponding to the first solid layer is employed to compute the Rayleigh dispersion curves (including normal modes and leaky modes) shown in Figure 14. In this case there are many PL modes, which are likewise approximated by the acoustic normal modes. Same with the OP modes for the near-surface model in case 1, the OP modes for the shallow water model are also reverse continuations of the normal modes behind their cut-off frequencies.

Figure 15 is the attenuation diagram of the leaky modes in Figure 14. Once again, with the increasing frequency the attenuations of the leaky modes of the same order gradually decrease, and the attenuations of the PL modes are particularly small. Therefore, judging from the attenuation diagram alone we could predict that the leaky modes of phase velocities slightly larger than the maximum S-wave velocity and the PL modes are apt to appear on the dispersion spectrum. Nevertheless, we should bear in mind that, the excitation of modes also depends upon the source mechanism and the source-receiver configuration.

Figure 16 shows the dispersion spectrum when the source is just above the seafloor and the receiver is only 10 m beneath the surface. Superimposed on the spectrum are the normal modes and leaky modes, represented by solid dots and open circles respectively. The bright regions above the maximum shear-wave velocity agree very well with the computed PL leaky modes. We further notice that the energy of the leaky modes on the dispersion spectrum is evidently stronger than that of the normal modes. This situation does not change much with different source-receiver configurations (Figure 17) except when the receiver is just located on the seafloor, in which case a number of normal modes appear yet weakly on the dispersion spectrum. This phenomenon may be well accounted for by the concept of 'adaptive mode observers' proposed by Wu and Chen (2016), that is, one that is located at the depth where the eigen-displacements of a certain excited mode are significant, tends to feel the energy of this mode more strongly. Moreover, for a shallow-water model whose maximum shear velocity is still lower than the sound velocity in the water, the energies of all of the normal modes are trapped mainly in the seafloor (Wu et al., 2020).

The dispersion spectra with different source-receiver configurations are displayed in Figure 17. All the receiver depths are 10 m on the left panel and 40 m on the right panel, and the source depth ranges from 0 m to 200 m. As a whole, with the increase of the source depth leaky modes are excited more strongly, but when the source is too deep (see the case when the source is 200 m deep) the number of the excited leaky modes decreases instead. The excited modes are the most when the receiver is closer to the source, as is just discussed and can be well understood.

The eigen-displacements of the leaky modes are selectively computed at 31 Hz (Figure 18). Again, the oscillating character of the OP modes is distinct from that of the PL modes; the former have little energy in the water while the latter have significant energy in the upper region of the model. The discontinuity of the horizontal displacement across the ocean floor is seen for all of the modes. Because the PL modes in Figure 18 are found to have negligible energy below 200 m deep, this may account for the decrease in the number and the strength of the excited modes when the source depth is increased to 200 m (Figure 17). Were the source not a point source but a horizontal force source, some OP modes would be expected to appear on the spectrum, as illustrated by Znak et al. (2015).

4. Conclusions

Motivated by the two questions: a) under what conditions the leaky modes are favorably excited, and b) why many theoretically computed leaky modes are not present in the dispersion spectrum, we have investigated the excitation of leaky modes for multi-layered models in view of the attenuation and the eigen-displacements of the leaky modes.

First, based on the synthetic seismograms generated by the DWM and the NMM, we find that for a given model the contribution of leaky modes to the resultant seismograms depends upon the source mechanism and the source depth (the receiver is assumed to be on the surface). The source mechanism has little effect on the excitation of leaky modes to an observable level for a deep source, while this effect may be prominent for a shallow source; besides, for the same source mechanism, the source depth may play an important role in the excitation of leaky modes. Therefore, for a given model a deeper event tends to favor the excitation of leaky modes, and for a shallow source different source mechanisms may excite certain types of leaky modes.

Second, accurate computation of leaky modes is performed in the $(+,-)$ Riemann sheet. The leaky modes can be classified into two types: PL modes and OP modes. PL modes generally have little attenuation and, due to their being approximated by acoustic normal modes, they are more sensitive to P-wave velocities than to S-wave velocities and have a significant contribution to the early portion of the seismograms. In contrast, OP modes have larger attenuation but have a tendency to lower attenuation with the increasing frequency; moreover, they are more sensitive to shear-wave velocities and are reverse continuations of normal modes beyond their cut-off frequencies. These results may help explain why frequently present on the dispersion spectrum above the maximum shear-wave velocity are the PL modes and partial OP modes whose phase velocities are slightly larger than the maximum shear-wave velocity. Furthermore, the periodic appearance of the maximas and minimas of the attenuation curves of PL modes are held accountable for the pronounced tuning effect in the dispersion spectrum.

Third, a number of OP modes are absent on the dispersion spectrum, because these modes generally attenuate more heavily compared to PL modes, and also because the OP modes have little energy in the shallower subsurface regions in view of their eigen-displacements relative to those of PL modes. However, certain source mechanisms may still excite some OP modes for shallow sources.

In conclusion, judging from the attenuation and the eigen-displacements of leaky modes, we are greatly aided to analyze the dispersion spectrum. With the recent soaring interest in applying an array-based method to extract leaky-mode dispersion curves and in an attempt to invert the P-wave velocities (Li et al., 2021; Li et al., 2022), we are further served by this study to suitably select certain leaky modes combined with normal modes to perform joint inversion to obtain reliable P-wave velocity structure.

Acknowledgements

The authors wish to thank Dr. Zhengbo Li for sharing his ideas on some aspects of leaky modes. This research was funded by the National Natural Science Foundation of China (grant 41704041).

Open Research

All of the model data used in this study are explicitly shown or cited appropriately in the text. The computer codes for modeling the synthetic seismograms are available from the corresponding author upon reasonable request.

References

Aki, K., & Richards, P. G. (1980), *Quantitative Seismology: Theory and Methods*, W. H. Freeman, San Francisco.

Boiero, D., Wiarda, E., & Vermeer, P. (2013), Surface- and guided-wave inversion for near-surface modeling in land and shallow marine seismic data, *The Leading Edge*, *32*(6), 638-646, doi:10.1190/tle32060638.1.

Bouchon, M., & Aki, K. (1977), Discrete wavenumber representation of seismic source wave fields, *Bulletin of the Seismological Society of America*, *67*(2), 259-277.

Chen, W., & Chen, X. (2002), Modal solutions in stratified multi-layered fluid-solid half-space, *Science in China Series D: Earth Sciences*, *45*(4), 358-365, doi:10.1360/02yd9037.

Chen, X. (1993), A systematic and efficient method of computing normal mode for multilayered half space, *Geophysical Journal International*, *115*(2), 391-409.

Chen, X. (1999), Seismogram synthesis in multi-layered half-space Part I. Theoretical formulations, *Earthquake research in China*, *13*(2), 149-174.

Chen, X., & Zhang, H. (2001), An Efficient Method for Computing Green's Functions for a Layered Half-Space at Large Epicentral Distances, *Bulletin of the Seismological Society of America*, *91*(4), 858-869, doi:10.1785/0120000113.

Cochran, M. D., Woeber, A. F., & De Bremaecker, J. C. (1970), Body waves as normal and leaking modes, 3. Pseudo modes and partial derivatives on the (+−) sheet, *Reviews of Geophysics and Space Physics*, *8*(2), 321-357.

Dainty, A. M. (1971), Leaking modes in a crust with a surface layer, *Bulletin of the Seismological Society of America*, *61*(1), 93-107.

De Bremaecker, J. C. (1967), Body waves as normal and leaking modes, Part I: Introduction, *Bulletin of the Seismological Society of America*, *57*(2), 191-198.

Fujita, M., & Nishimura, K. (1991), Estimation of crustal structure from observed group velocities of PL-waves in Japan, *Pure and applied geophysics*, *137*(3), 233-249, doi:https://doi.org/10.1007/BF00876990.

Furumura, T., & Kennett, B. L. N. (2018), Regional Distance PL Phase in the Crustal Waveguide—An Analog to the Teleseismic W Phase in the Upper-Mantle Waveguide, *Journal of Geophysical Research: Solid Earth*, *123*(5), 4007-4024, doi:https://doi.org/10.1029/2018JB015717.

Gao, L., Xia, J., & Pan, Y. (2014), Misidentification caused by leaky surface wave in high-frequency surface wave method, *Geophysical Journal International*, *199*(3), 1452-1462.

García-Jerez, A., & Sánchez-Sesma, F. J. (2015), Slowly-attenuating P-SV leaky waves in a layered elastic halfspace. Effects on the coherences of diffuse wavefields, *Wave Motion*, *54*, 43-57, doi:https://doi.org/10.1016/j.wavemoti.2014.11.010.

Gilbert, F. (1964), Propagation of transient leaking modes in a stratified elastic waveguide, *reviews of geophysics*, *2*(1), 123-153.

Gilbert, F., & Laster, S. J. (1962), Experimental investigation of PL modes in a single layer, *Bulletin of the Seismological Society of America*, *52*(1), 59-66, doi:10.1785/bssa0520010059.

Haddon, R. A. W. (1984), Computation of synthetic seismograms in layered earth models using leaking modes, *Bulletin of the Seismological Society of America*, *74*(4), 1225-1248.

Haddon, R. A. W. (1986), Exact evaluation of the response of a layered elastic medium to an explosive point source using leaking modes, *Bulletin of the Seismological Society of America*, *76*(6), 1755-1775.

Haddon, R. A. W. (1987), Response of an oceanic wave guide to an explosive point source using leaking modes, *Bulletin of the Seismological Society of America*, *77*(5), 1804-1822.

Haskell, N. A. (1966), The leakage attenuation of continental crustal P waves, *Journal of Geophysical Research*, *71*, 3955-3967.

He, Y., Chen, W., & Chen, X. (2006), Normal mode computation by the generalized reflection-transmission coefficient method in planar layered half space, *Chinese Journal of Geophysics*, *49*(4), 1074-1081.

Ibrahim, A.-B. K. (1969), Leaking and normal modes as a means to determine crust-upper mantle structure for different paths to Sweden, *Bulletin of the Seismological Society of America*, *59*(4), 1695-1712, doi:10.1785/bssa0590041695.

Laster, S. J., Foreman, J. G., & Linville, F. (1965), Theoretical investigations of modal seismograms for a layer over a half-space, *Geophysics*, *30*(4), 571-596.

Li, Z., & Chen, X. (2020), An Effective Method to Extract Overtones of Surface Wave From Array Seismic Records of Earthquake Events, *Journal of Geophysical Research: Solid Earth*, *125*(3), e2019JB018511. https://doi.org/018510.011029/012019JB018511.

Li, Z., Shi, C., & Chen, X. (2021), Constraints on Crustal P Wave Structure With Leaking Mode Dispersion Curves, *Geophysical Research Letters*, *48*(20), e2020GL091782, doi:https://doi.org/10.1029/2020GL091782.

Li, Z., Shi, C., Ren, H., & Chen, X. (2022), Multiple Leaking Mode Dispersion Observations and Applications From Ambient Noise Cross-Correlation in Oklahoma, *Geophysical Research Letters*, *49*(1), e2021GL096032, doi:https://doi.org/10.1029/2021GL096032.

Ma, D.-y., Zhang, Y.-x., Xie, Z.-n., Gao, J.-h., & Yin, J.-w. (2019), Sea-ice thickness measurement based on ice layer waveguide theory, *Technical Acoustics*, *38*(4 Pt.2), 479-482, doi:10.26914/c.cnkihy.2019.062497.

Oliver, J. (1961), On the long period character of shear waves, *Bulletin of the Seismological Society of America*, *51*(1), 1-12, doi:10.1785/bssa0510010001.

Oliver, J. (1964), Propagation of PL waves across the United States, *Bulletin of the Seismological Society of America*, *54*(1), 151-160.

Oliver, J., & Major, M. (1960), Leaking modes and the PL phase, *Bulletin of the Seismological Society of America*, *50*(2), 165-180.

Phinney, R. A. (1961), Leaking modes in the crustal waveguide, Part 1. The oceanic PL wave, *Journal of Geophysical Research*, *66*(5), 1445-1469.

Radovich, B. J., & De Bremaecker, J. C. (1974), Body waves as normal and leaking modes - leaking modes of Love waves, *Bulletin of the Seismological Society of America*, *64*(2), 301-306.

Rosenbaum, J. H. (1960), The long time response of a layered elastic medium to explosive sound, *Journal of Geophysical Research*, *65*(5), 1577-1613.

Roth, M., & Holliger, K. (1999), Inversion of source-generated noise in high-resolution seismic data, *The Leading Edge*, *18*(12), 1402-1406, doi:10.1190/1.1438230.

Roth, M., Holliger, K., & Green, A. G. (1998), Guided waves in near-surface seismic surveys, *Geophysical Research Letters*, *25*(7), 1071-1074.

Shen, W., & Ritzwoller, M. H. (2016), Crustal and uppermost mantle structure beneath the United States, *Journal of Geophysical Research: Solid Earth*, *121*(6), 4306-4342, doi:https://doi.org/10.1002/2016JB012887.

Sommville, O. (1930), A propos d'une onde longue dans la première phase de quelques séismogrammes, *Gerlands Beitraege zur Geophysik*, *27*, 437-442.

Stalmach, D. M., & De Bremaecker, J. C. (1973), Body waves as normal and leaking modes: Dispersion and excitation on the (+−) sheet, *Bulletin of the Seismological Society of America*, *63*(3), 995-1011.

Su, S. S., & Dorman, J. (1965), The use of leaking modes in seismogram interpretation and in studies of crust-mantle structure, *Bulletin of the Seismological Society of America*, *55*(6), 989-1021.

Wang, C. Y., & Herrmann, R. B. (1980), A numerical study of P-, SV-, and SH-wave generation in a plane layered medium, *Bulletin of the Seismological Society of America*, *70*(4), 1015-1036.

Wang, J., Wu, G., & Chen, X. (2019), Frequency-Bessel transform method for effective imaging of higher-mode Rayleigh dispersion curves from ambient seismic noise data, *Journal of Geophysical Research: Solid Earth*, *124*(4), 3708-3723.

Watson, T. H. (1972), A real frequency, complex wavenumber analysis of leaking modes, *Bulletin of the Seismological Society of America*, *62*(1), 369-384.

Wu, B., & Chen, X. (2016), Stable, accurate and efficient computation of normal modes for horizontal stratified models, *Geophysical Journal International*, *206*(2), 1281-1300.

Wu, B., & Chen, X. (2017), Accurate computation of leaky modes for anomalous layered models, *Annals of Geophysics*, *60*(6), S0663, doi:10.4401/ag-7477.

Wu, B., & Chen, X. (2022), A Versatile Solver of the Normal Modes for Horizontal Stratified Complicated Models, *Seismological Research Letters*, *93*(3), 1852-1867, doi:10.1785/0220210266.

Wu, B., Li, Z., & Chen, X. (2020), Some aspects of dispersion calculation for models with surficial fluid layers, paper presented at Annual Meeting of Chinese Geoscience Union (CGU), Chongqing, 2020-10-18.

Znak, P., Kashtan, B., & Bakulin, A. (2015), Guided Waves and Rayleigh Leaking Modes With Outpost Algorithm, paper presented at 77th EAGE Conference and Exhibition 2015, IFEMA Madrid, Spain, 1-4 June 2015.

Table 1. Source parameters.

Fault type	Rake (°)	Dip (°)	Strike (°)	Azimuth (°)
Strike slip	180	90	45	30
Dip slip	90	45	45	30

Table 2. A near surface model, taken from Roth and Holliger (1999).

Layer No.	Thickness (m)	ρ (g/cm ^{3})	β (m/s)	α (m/s)
1	10	1.6	330	1100
2	∞	2.0	540	1800

Table 3. A shallow water model.

Layer No.	Thickness (m)	ρ (g/cm ^{3})	β (m/s)	α (m/s)
1	40	1.0	0	1500
2	40	1.5	600	1700
3	100	1.8	900	2300
4	∞	2.0	1200	3000

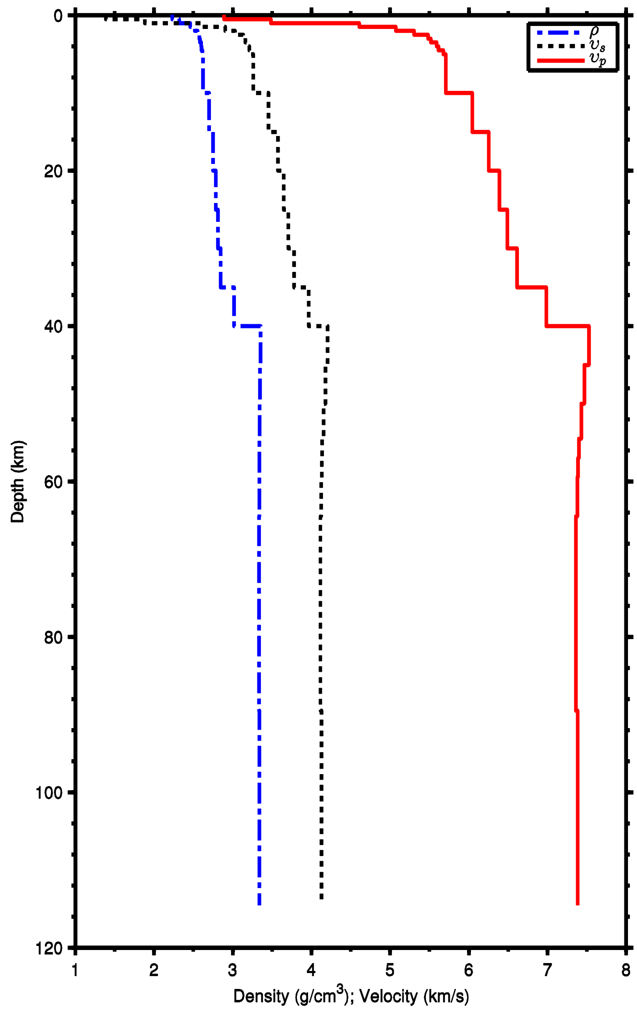

Figure 1. The crust-upper mantle model modified from Shen and Ritzwoller (2016).

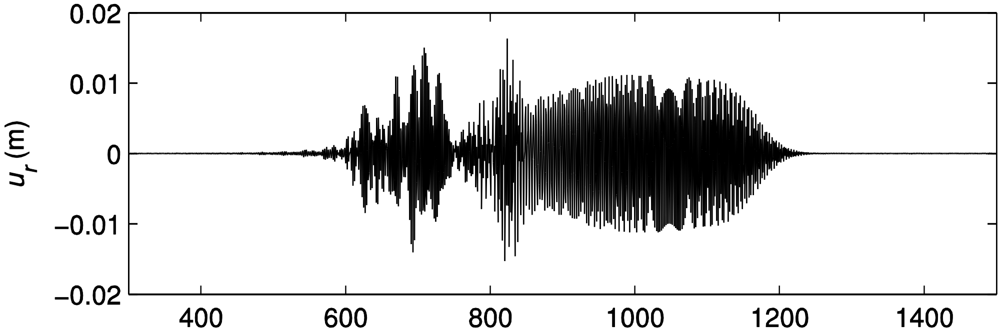
0.02
0.01
0
−0.01
−0.02
u_r (m)
400
600
800
1000
1200
1400

(A)

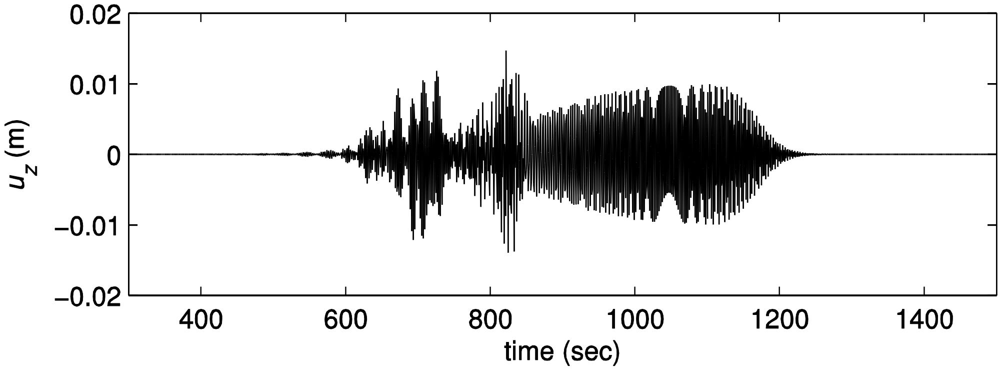
0.02
0.01
0
−0.01
−0.02
u_z (m)
400
600
800
1000
1200
1400
time (sec)

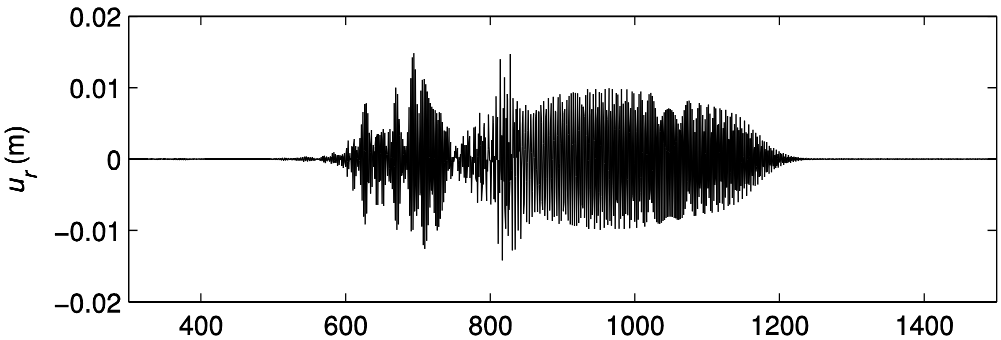
0.02
0.01
0
−0.01
−0.02
u_r (m)
400
600
800
1000
1200
1400

(B)

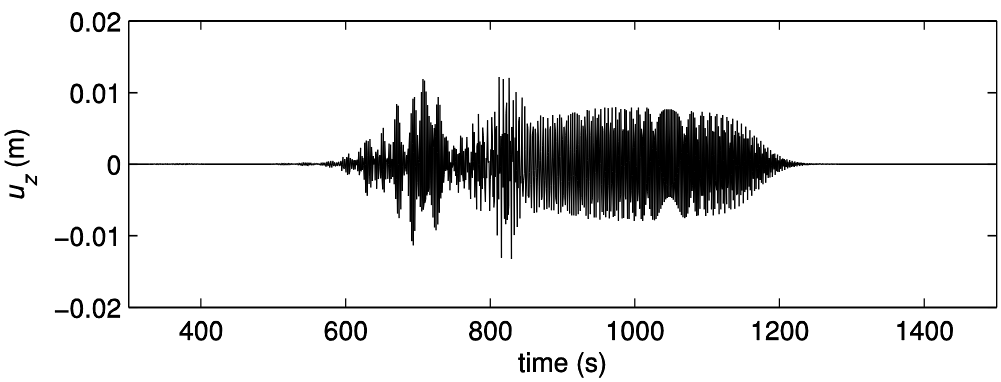
0.02
0.01
0
-0.01
−0.02
u_z (m)
400
600
800
1000
1200
1400
time (s)

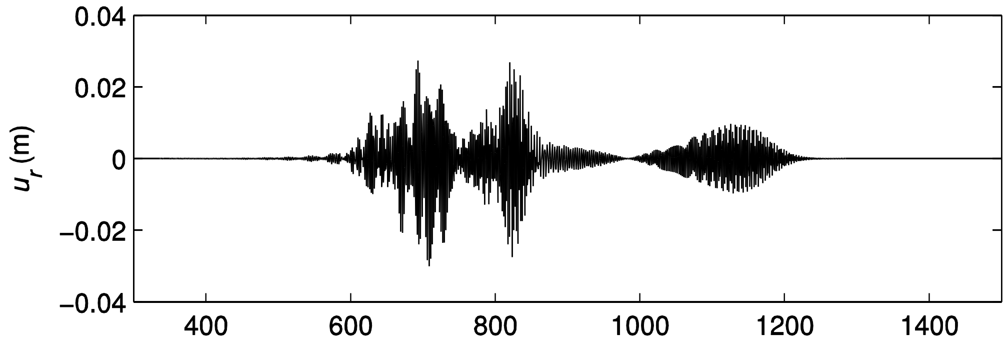

(C)

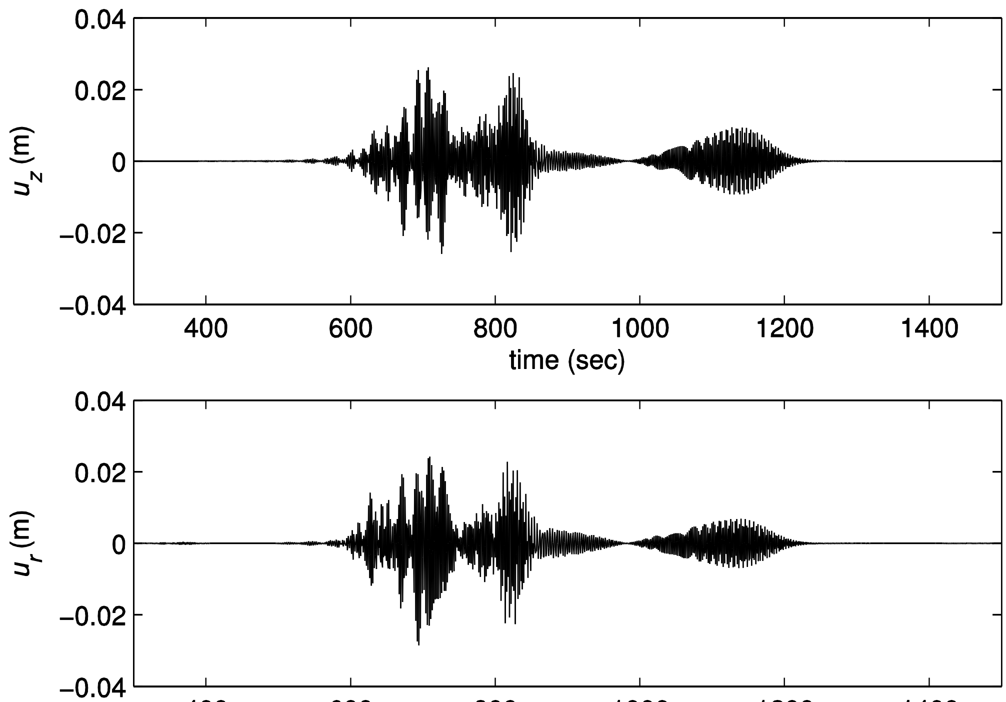

(D)

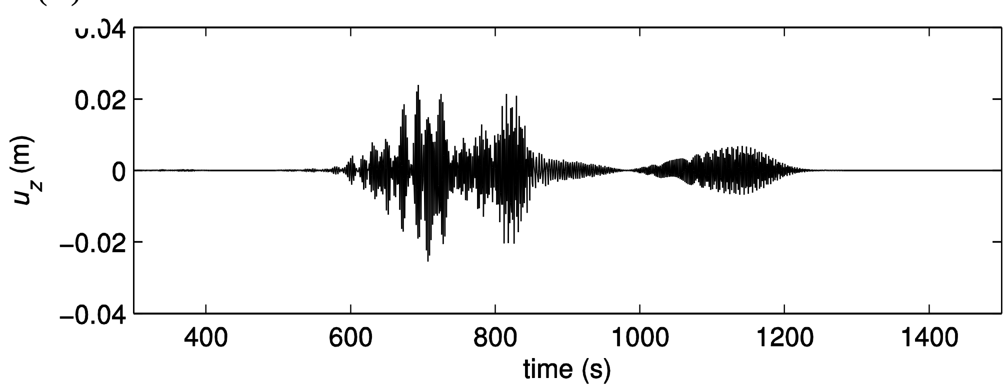

Figure 2. The synthetic seismograms (the radial component u_r and the vertical component u_z) for the seismic depth 0.5 km for the strike-slip (A, B) and the dip-slip (C, D) sources, computed by the NMM (A, C) and the DWM (B, D), respectively. The epicentral distance is 2000 km, and the time duration is 3000 s. The Hanning taper is applied to 0.01-0.55 Hz.

(A)

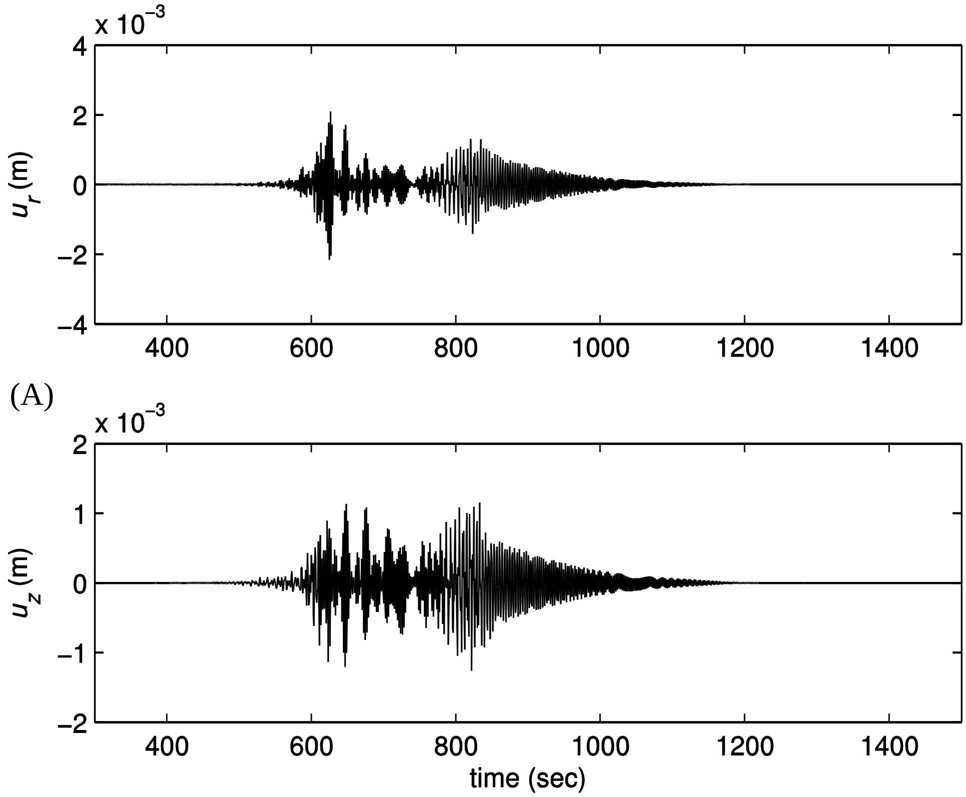

(B)

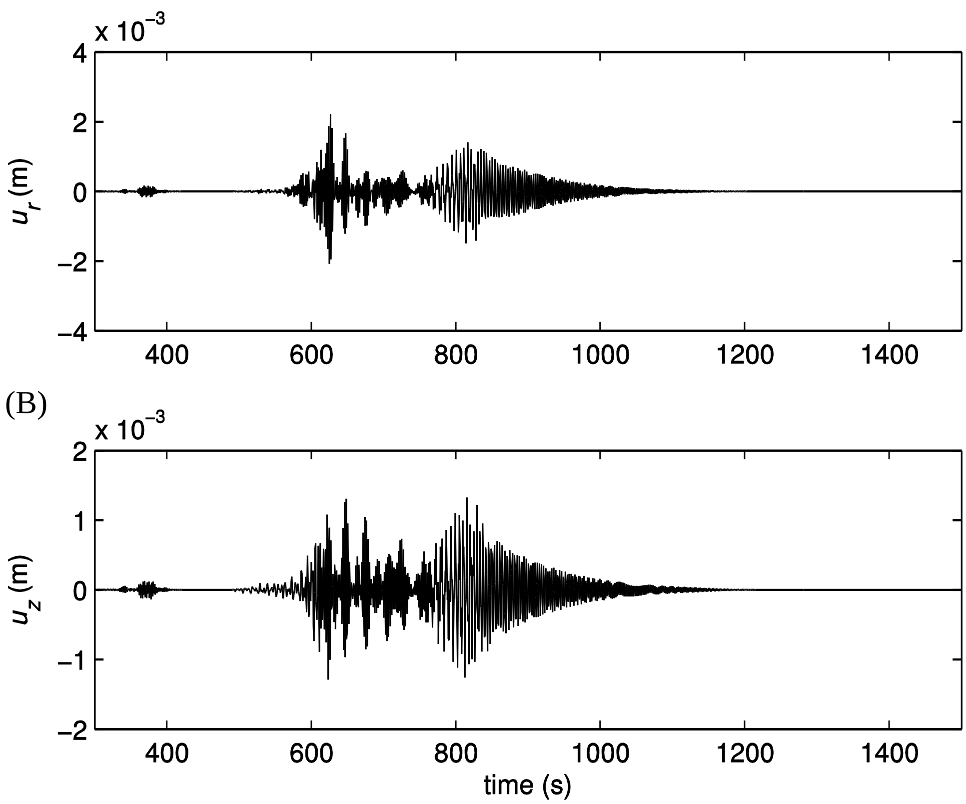

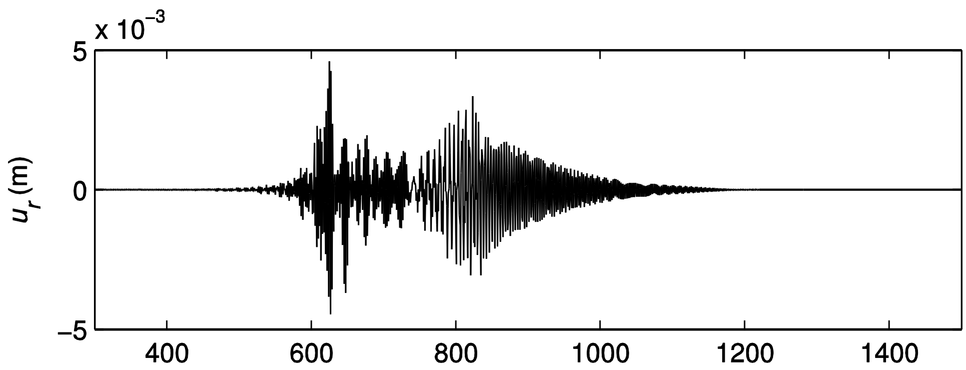

(C)

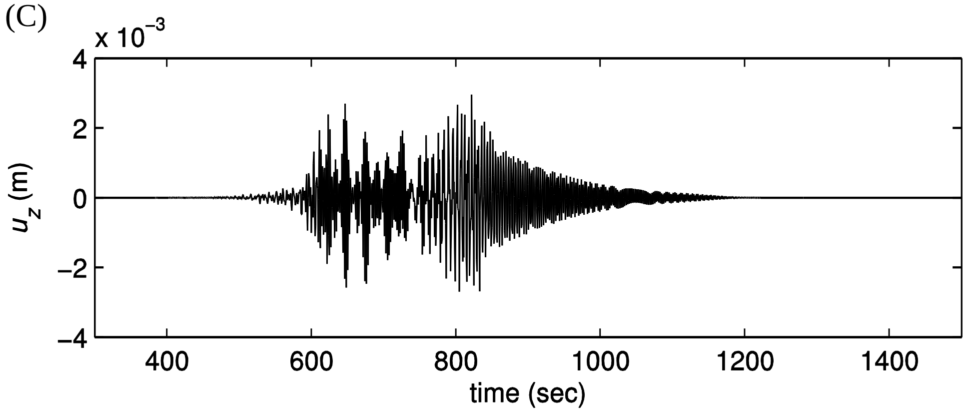

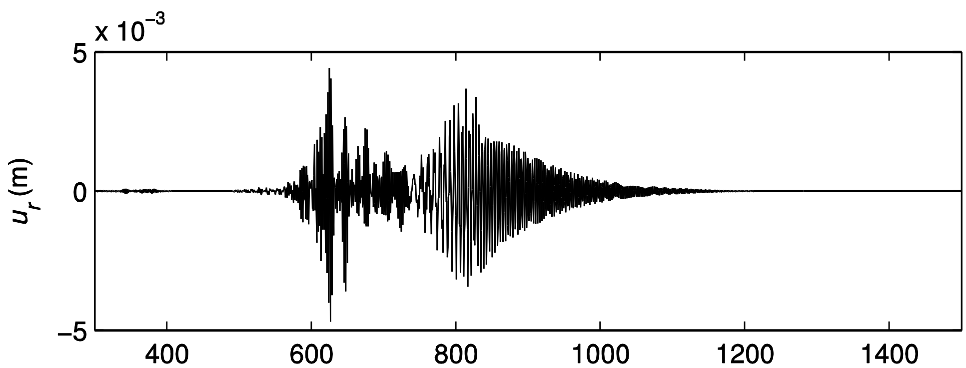

(D)

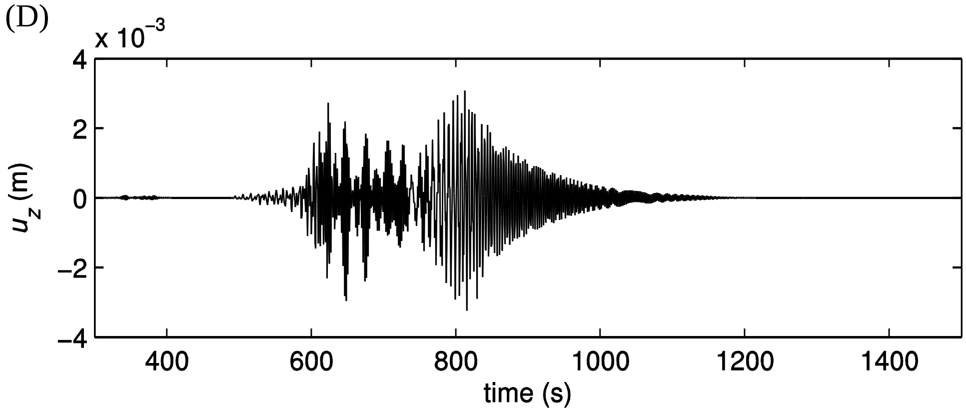

Figure 3. Same as Figure 2, except the source depth is 8 km.

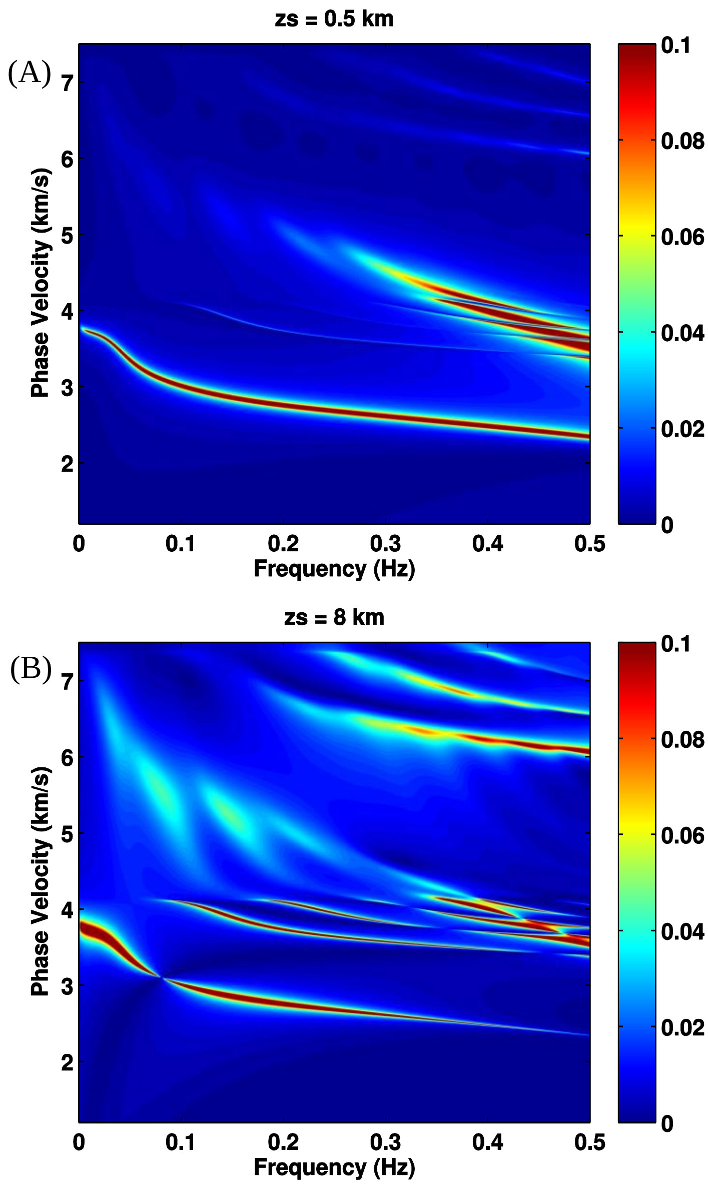

Figure 4. The theoretical dispersion spectra computed from the kernel function: (A) source depth $z_s = 0.5$ km; (B) source depth $z_s = 8$ km.

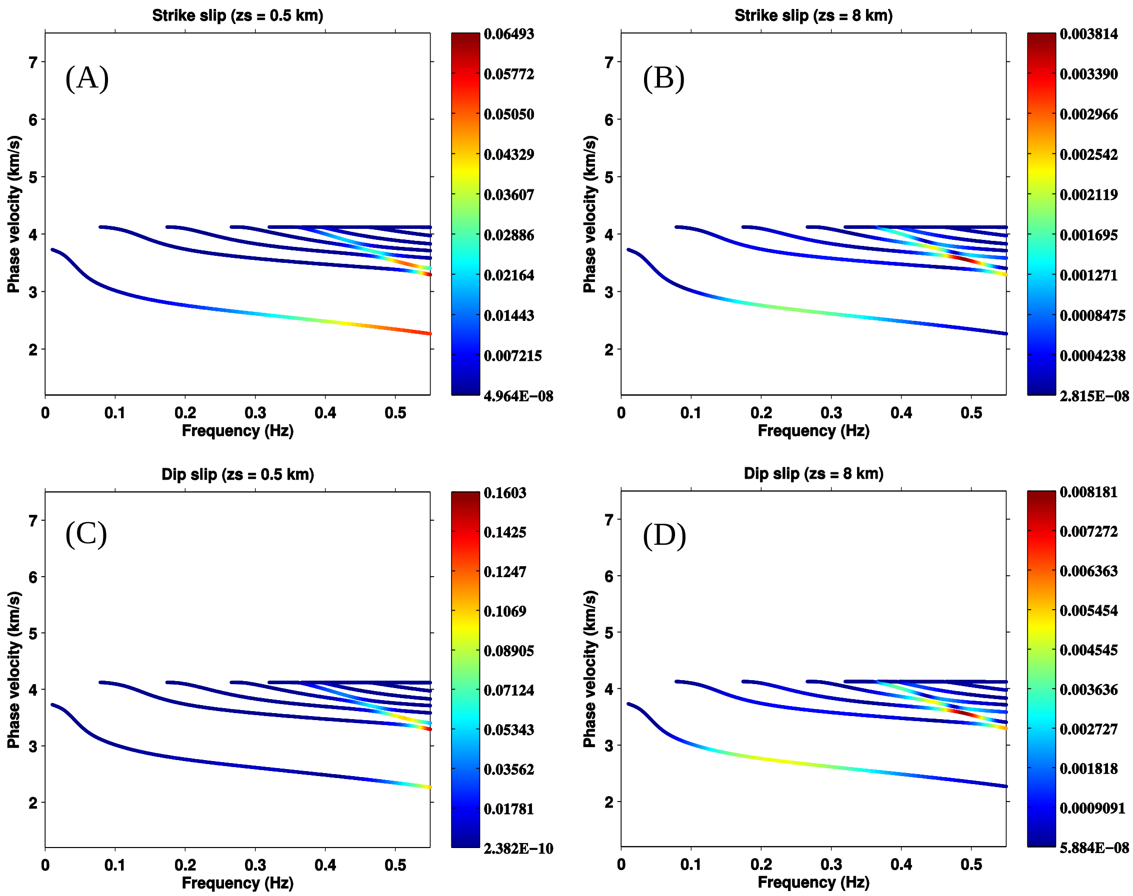

Figure 5. The diagrams of the excited strength of the normal modes for the model shown in Figure 1: (A) strike-slip source with depth 0.5 km; (B) strike-slip source with depth 8 km; (C) dip-slip source with depth 0.5 km; (D) dip-slip source with depth 8 km.

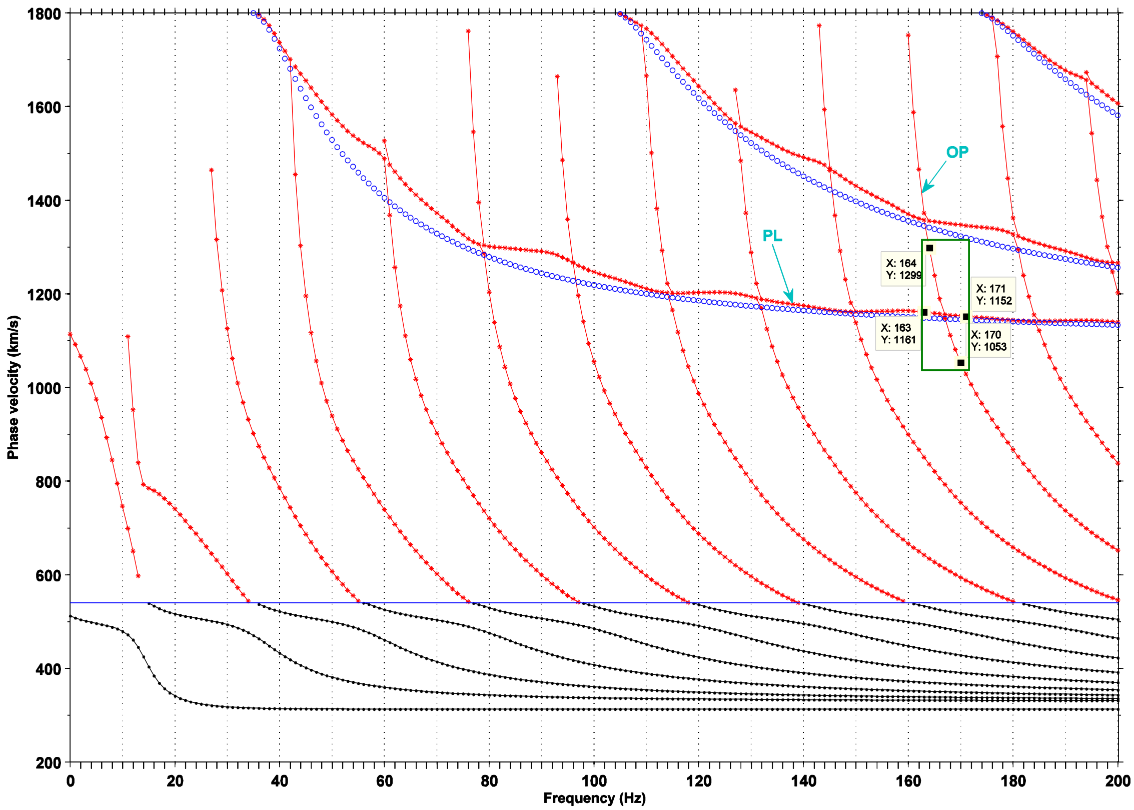

Figure 6. Dispersion curves of normal modes (black dots) and leaky modes (red dots) for the model shown in Table 2. Two distinct families of modes – PL modes and OP modes – are separately indicated. The horizontal blue line represents the maximum shear-wave velocity. The acoustic normal modes (blue open circles) are superimposed for comparison with PL modes. The eigen-displacements of the leaky modes in the green rectangle would then be calculated and plotted.

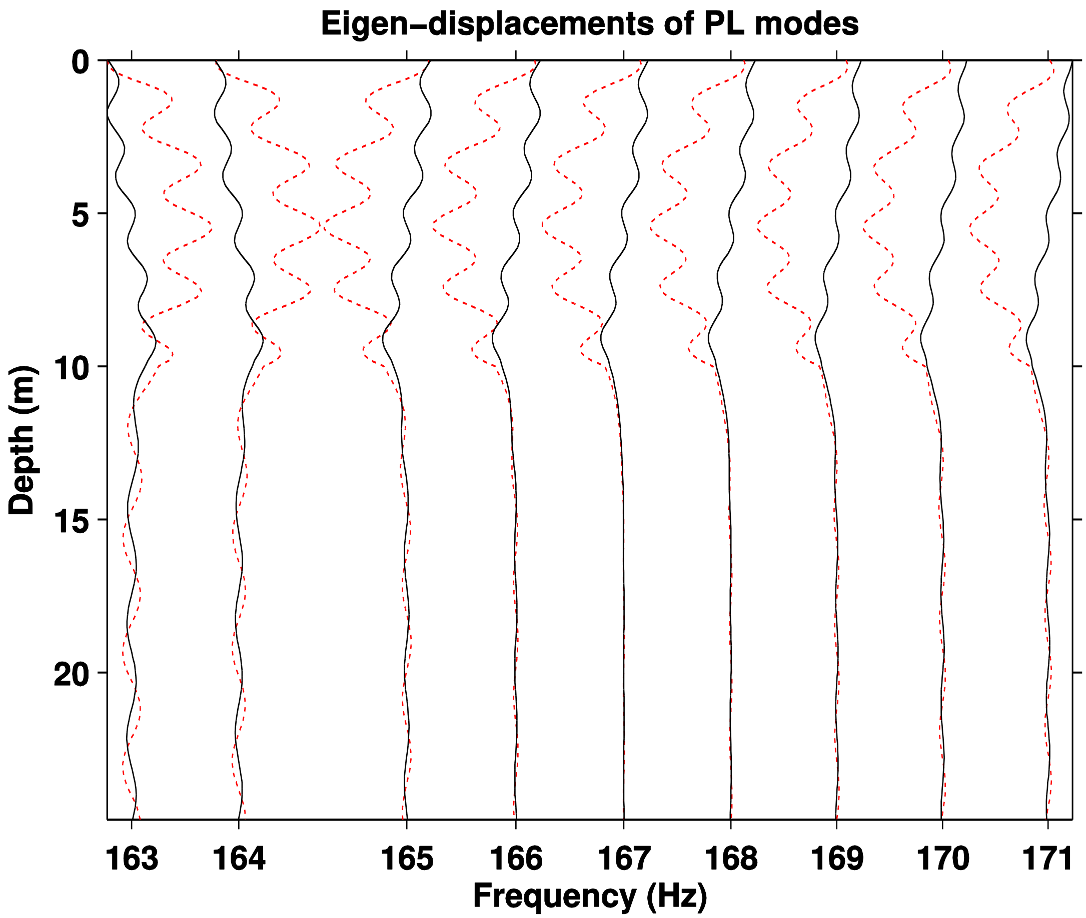

Figure 7. The eigen-displacements (real parts) of PL modes in the rectangular box in Figure 6. The vertical and horizontal displacements are denoted by black solid line and red dotted line, respectively.

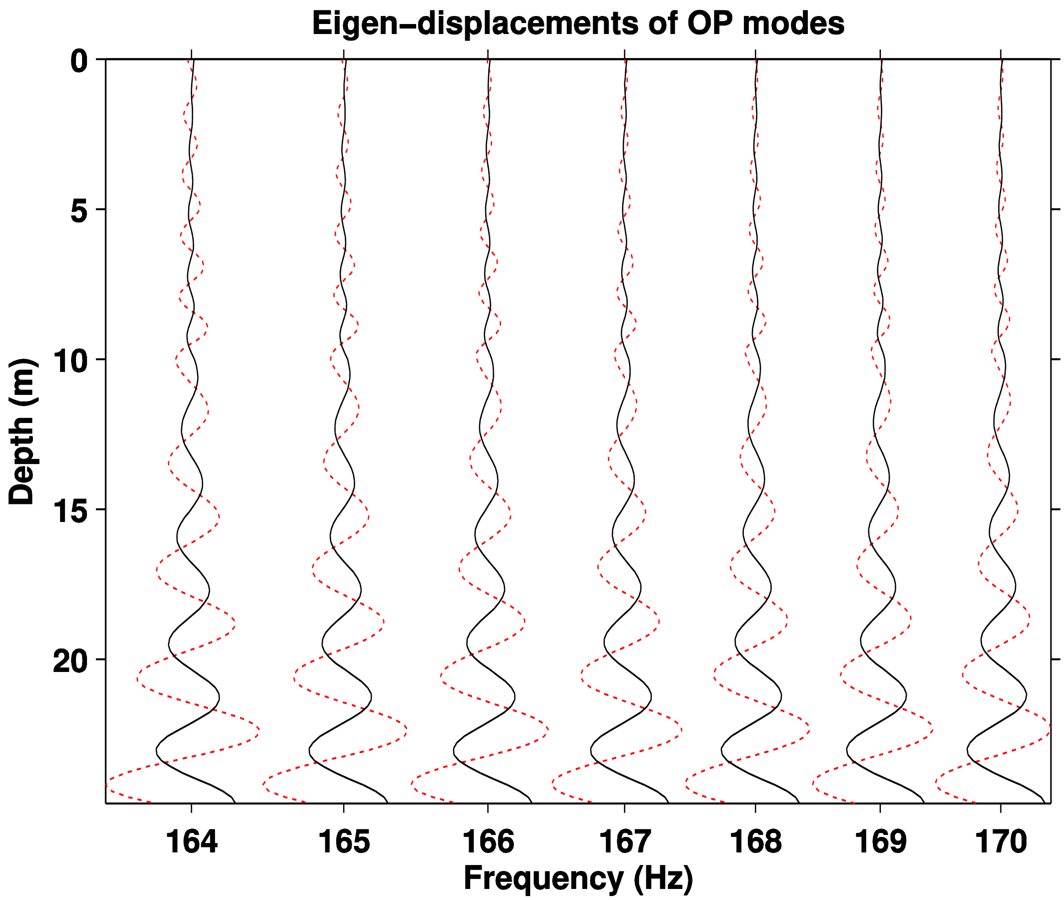

Figure 8. The eigen-displacements (real parts) of OP modes in the rectangular box in Figure 6 (the same denotation of line types and color as Figure 7).

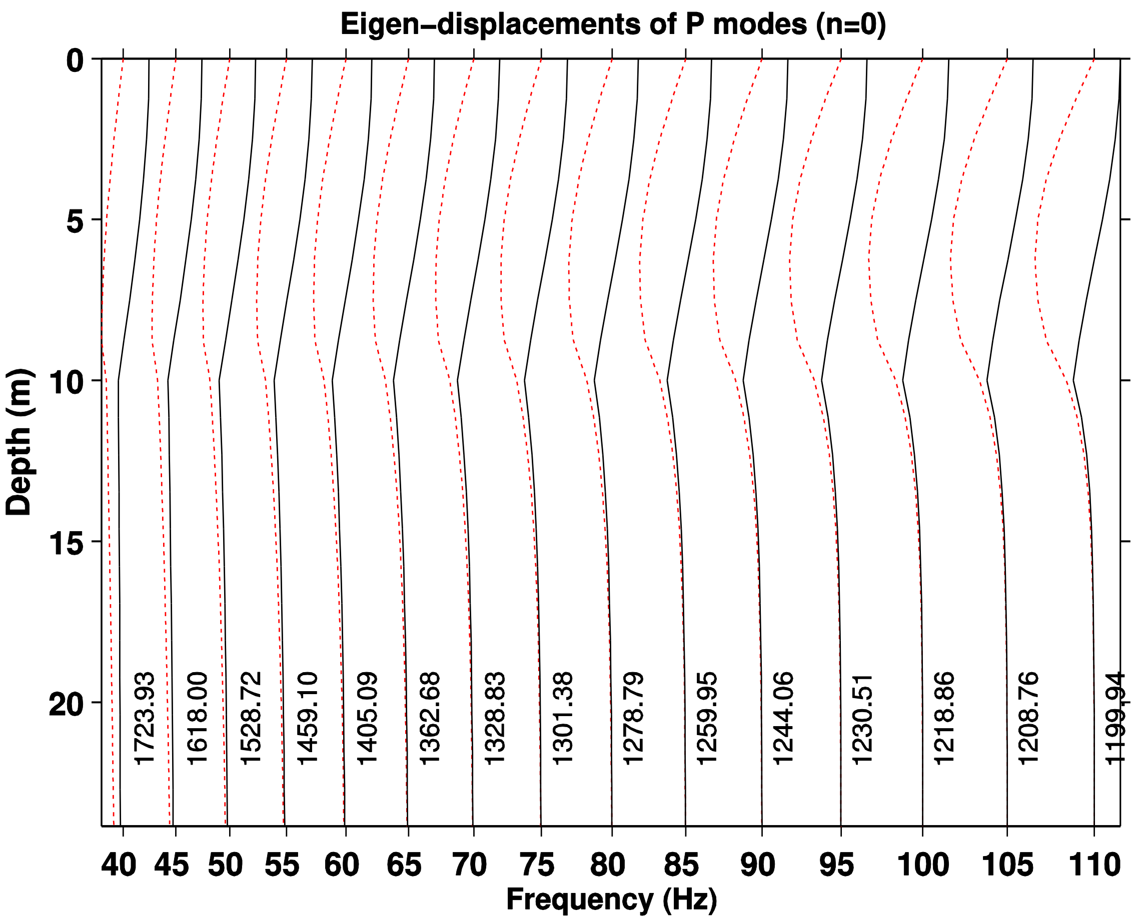

Figure 9. The eigen-displacements of the fundamental ($n = 0$) acoustic normal modes (P modes) at selected frequencies for the model shown in Table 2 but with vanishing values of shear velocities. The phase velocity of each mode is labeled appropriately. The denotation of line types and colors is the same as Figure 7.

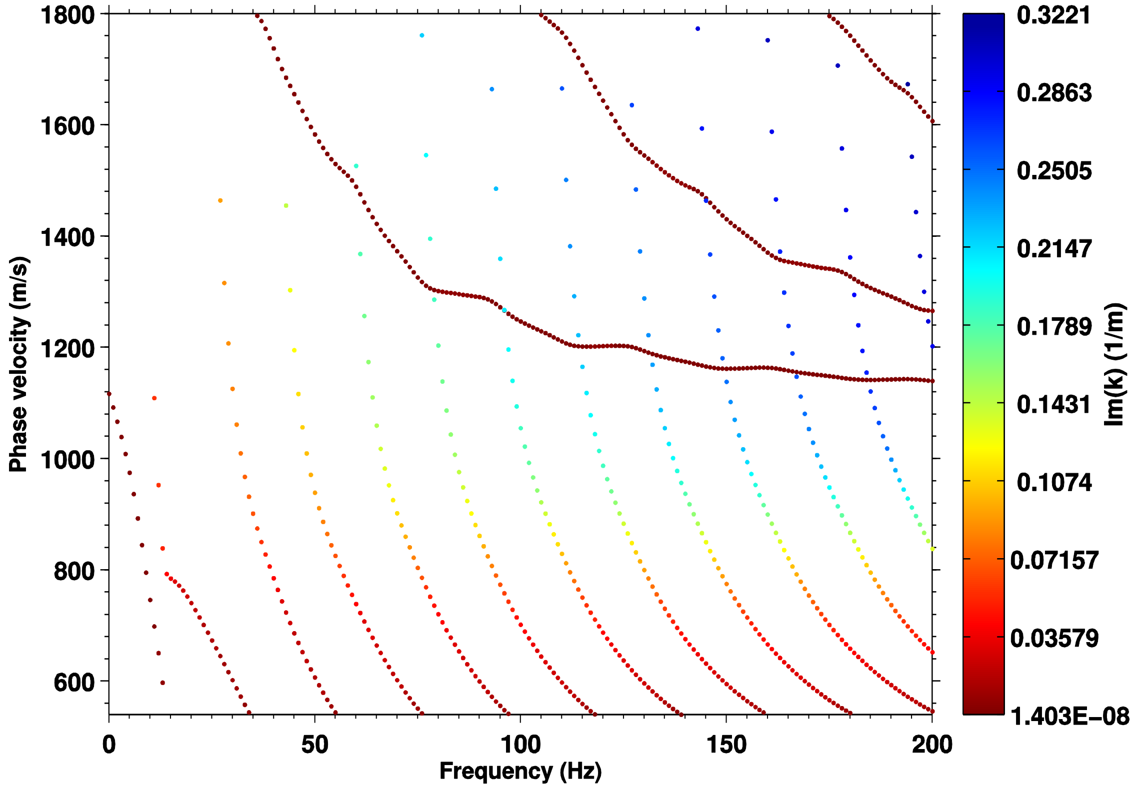

Figure 10. The attenuation of the leaky modes shown in Figure 6.

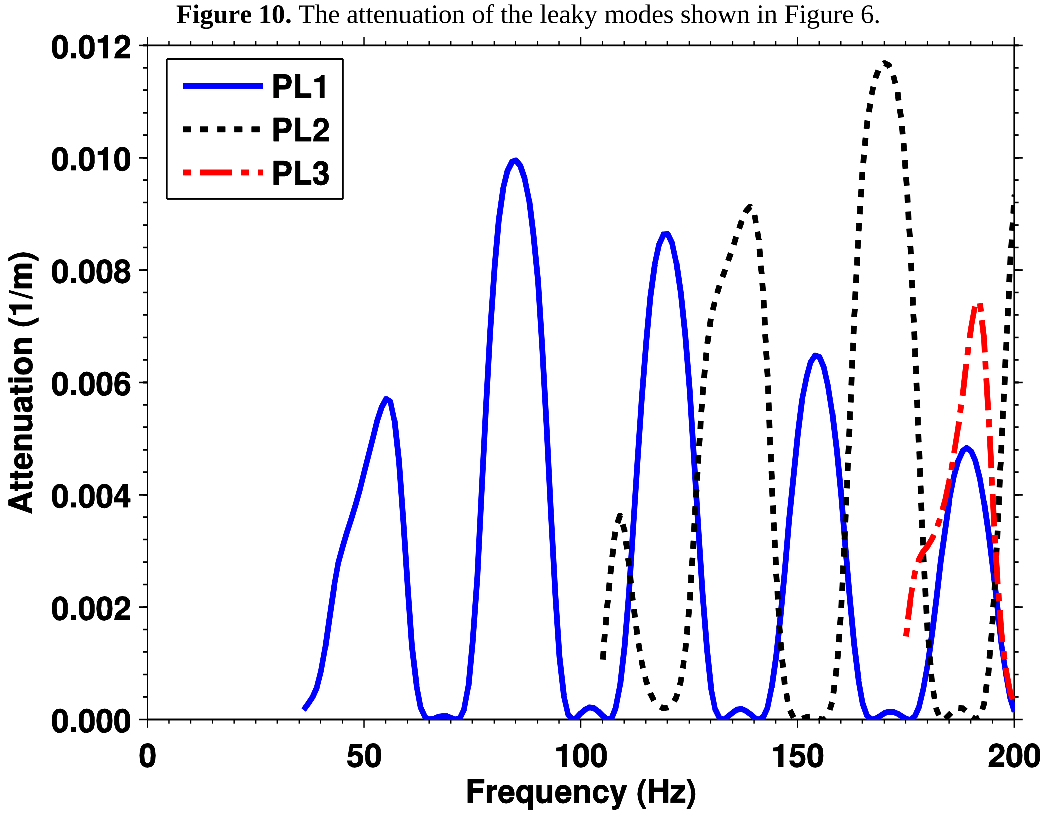

Figure 11. The attenuation curves of the three PL modes shown in Figure 6.

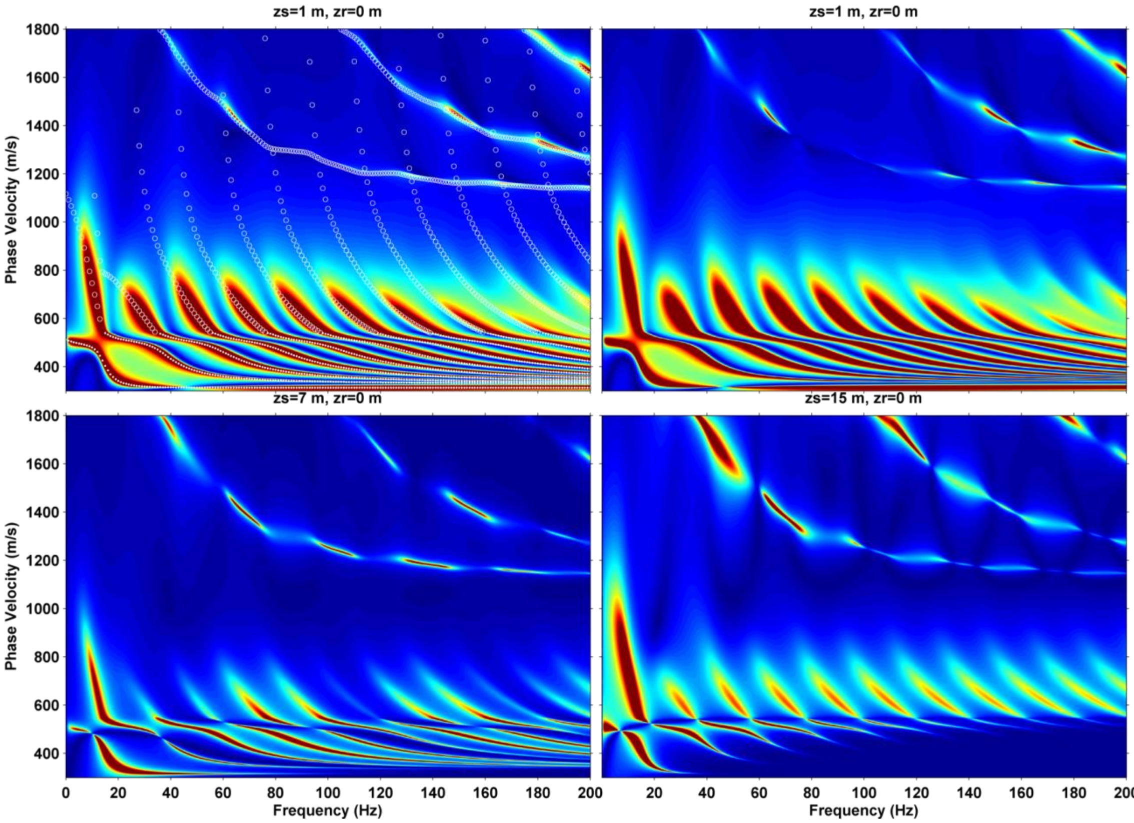

Figure 12. The dispersion spectrum computed for the near surface model (Table 2). The corresponding source depth and receiver depth are indicated above each subplot. The normal modes (solid dots) and leaky modes (open circles) are superimposed on the first subplot for reference.

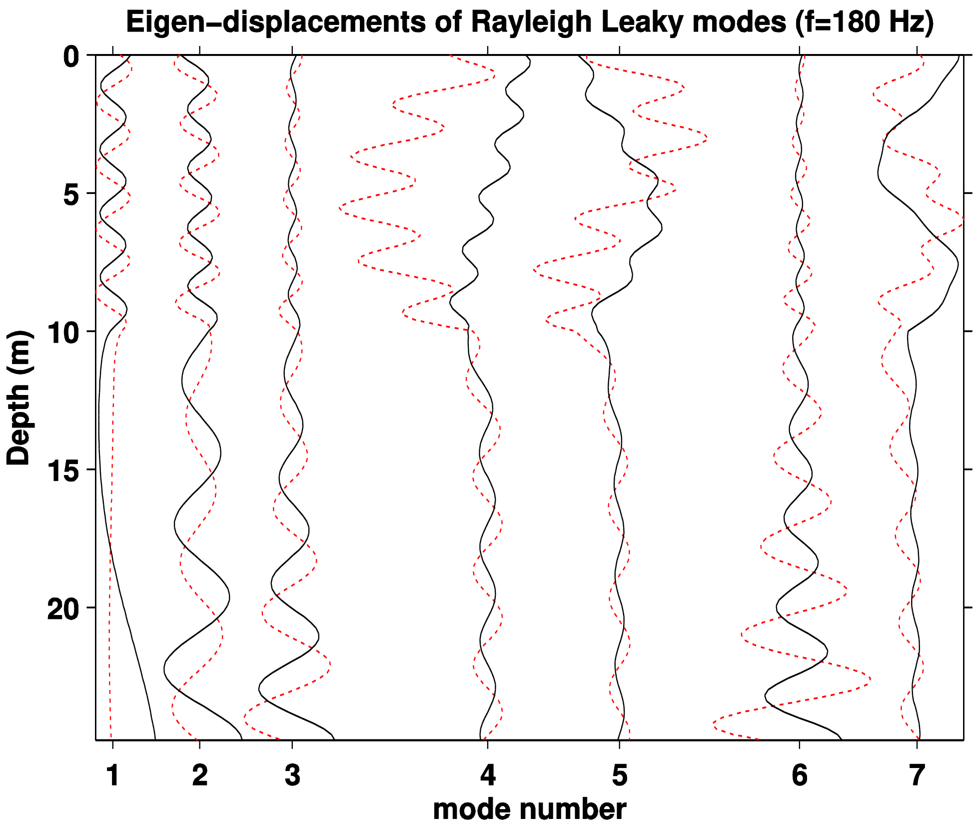

Figure 13. The eigen-displacements (real parts) of the leaky modes for the near surface model (Table 2) at 180 Hz (the same denotation of line types and color as Figure 7).

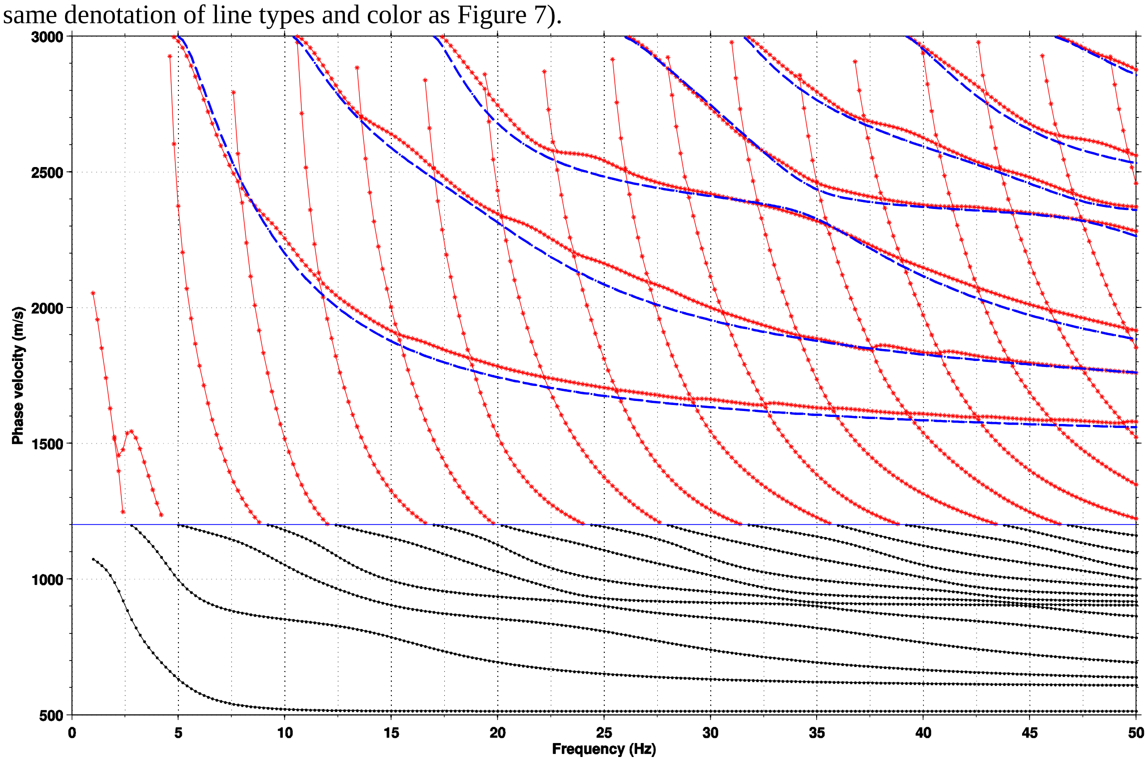

Figure 14. Dispersion curves of normal modes (black dots) and leaky modes (red dots) for the model shown in Table 3 (the same denotation of line types and color as Figure 6).

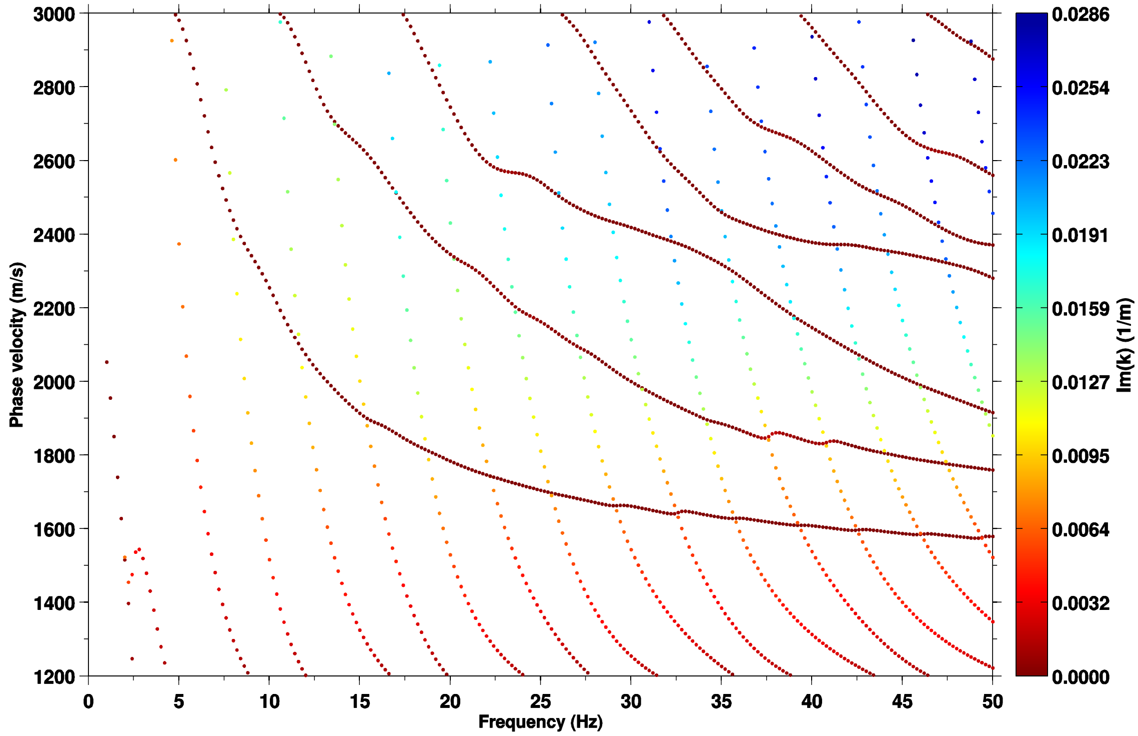

Figure 15. The attenuation of the leaky modes shown in Figure 14.

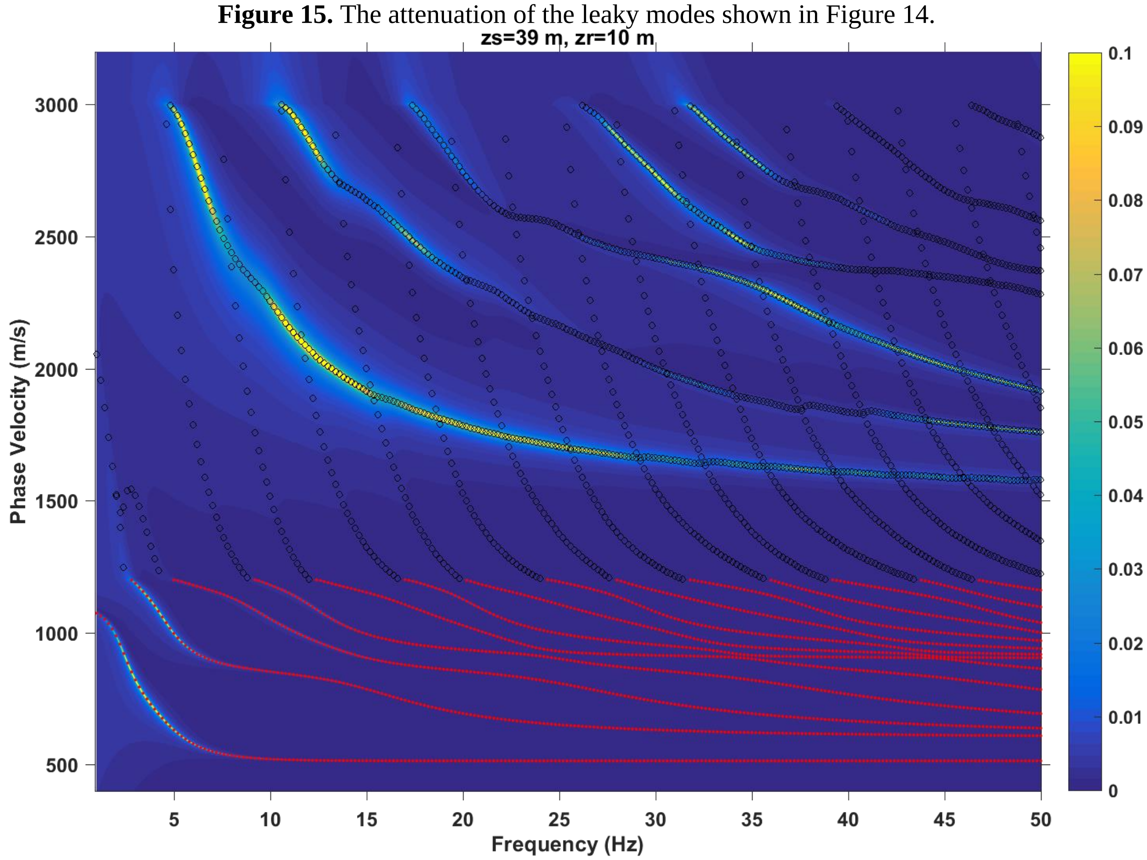

Figure 16. The dispersion spectrum computed for the shallow water model (Table 3). The corresponding source depth and receiver depth are labeled above. The normal modes (solid dots) and leaky modes (open circles) are superimposed for reference.

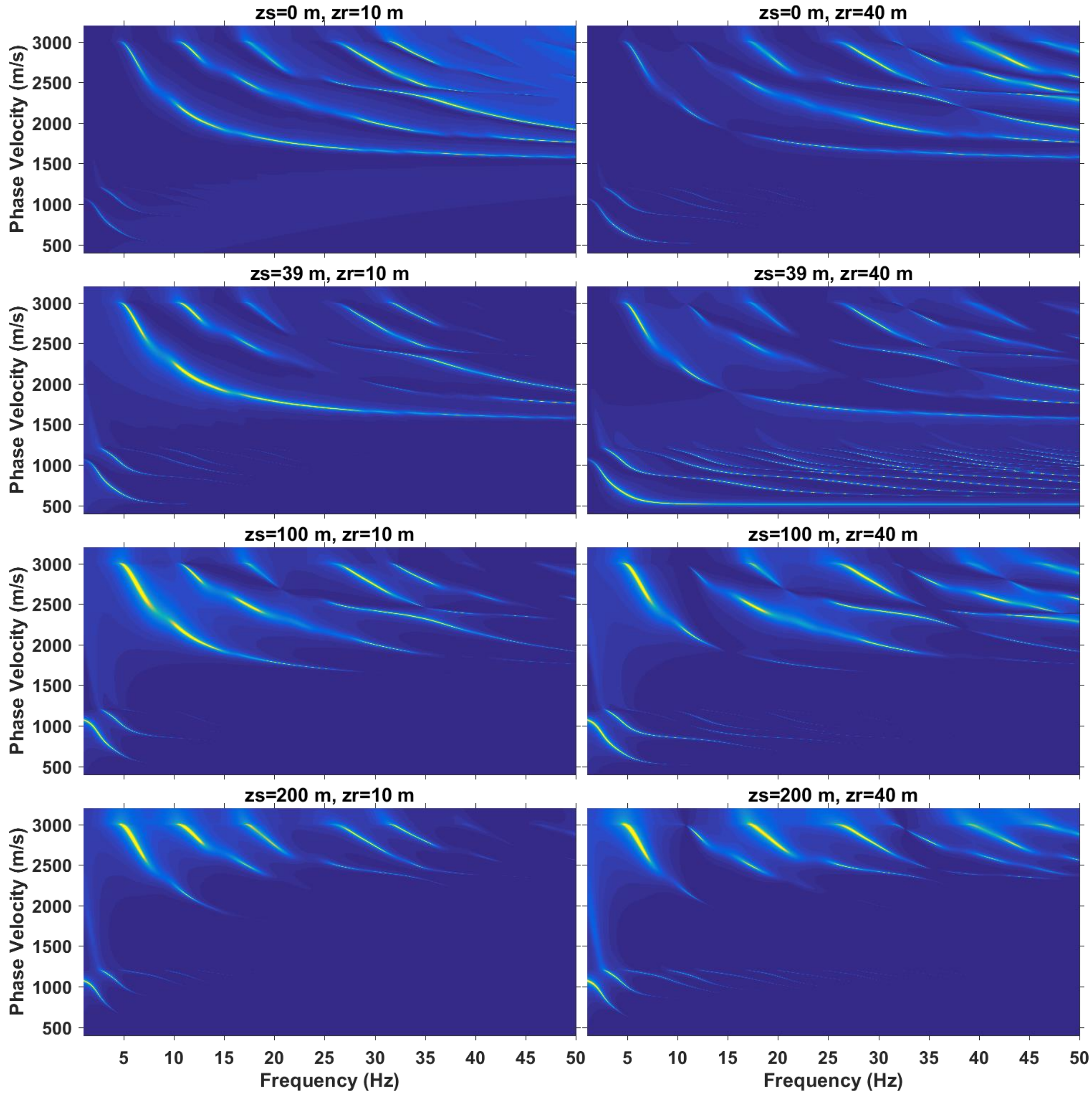

Figure 17. The dispersion spectrum for the shallow water model (Table 3) at different source depths (0, 39, 100 and 200 m) and receiver depths (10 and 40 m).

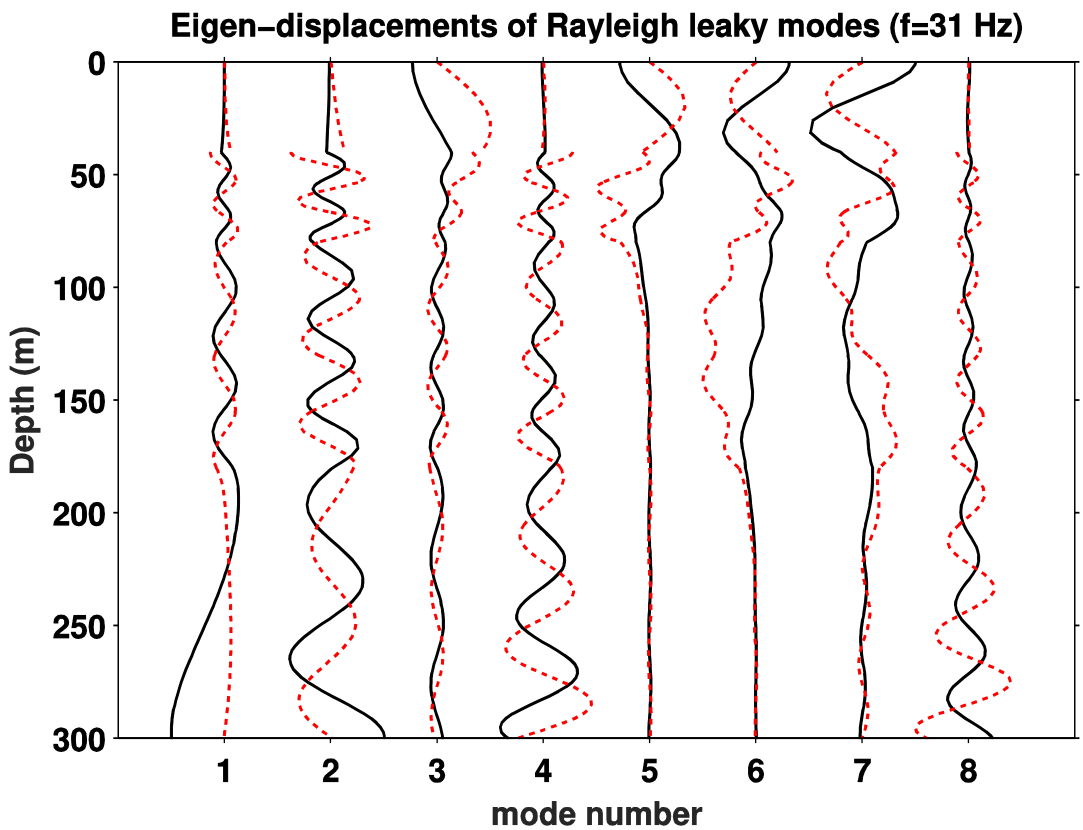

Figure 18. The eigen-displacements (real parts) of the leaky modes for the shallow water model (Table 3) at 31 Hz (the same denotation of line types and color as Figure 7).